

## Modeling the Plasma-Sheath Boundary for a Cylindrical Probe in Electronegative Plasmas

T. H. CHUNG\*

*Department of Physics, Dong-A University, Busan 604-714*

(Received 8 January 2009)

The spatial distributions of the electric potential and of the velocity and density of positive ions are calculated in the surroundings of a negatively-biased cylindrical probe immersed in an electronegative plasma. The model equations are solved on the scale of the ionization length. The position of the sheath edge, the positive ion velocity at the sheath edge and the positive ion current collected by the probe are determined and compared with the values obtained by using analytic (or scaling) formulas. Effects of control parameters on the positive ion velocity at the sheath edge and on the sheath width (thus, on the positive ion current) are investigated. A larger thermal motion of positive (and negative) ions causes the positive ion velocity at the sheath edge to increase, the sheath to increase and the positive ion current collected by the probe to increase. An increase in the number of collisions causes the positive ion velocity at the sheath edge to decrease and the sheath to decrease, resulting in a decrease in the positive ion current. An increase in the electronegativity causes the positive ion velocity at the sheath edge to decrease and the sheath width to decrease, resulting in an increase in the positive ion current. As the value of the non-neutrality parameter  $q$  increases, the positive ion current collected by the probe increases. We observed that the deviation from the plasma approximation became significant even at  $q = 0.006$ , which is a typical case for high-density electronegative plasmas and that the plasma approximation was no longer valid except for plasmas with the  $q$  less than 0.0005.

PACS numbers: 52.20.ch, 52.25.-b, 52.80.Pi

Keywords: Cylindrical electrostatic probe, Electronegative plasma, Sheath, Fluid model

### I. INTRODUCTION

There has been growing interest in electronegative plasmas because electronegative gases, such as oxygen, chlorine and  $SF_6$ , have been used extensively for many applications of plasma processing. Some important issues in electronegative plasmas include the problem of determining the electronegativity of the plasma, the sheath structure and the spatial distribution of plasma species [1–3].

If the electronegativity of a discharge is to be determined, the densities of electrons and negative ions have to be measured. A Langmuir probe can be applicable for this purpose. For an electronegative plasma, a careful interpretation of the  $I - V$  data of the probe is required [4,5]. A comparison of the experimental  $I - V$  curve of the Langmuir probe with the theoretical  $I - V$  curve can give a useful method of determining the plasma parameters. In order to construct a theoretical  $I - V$  curve for the cylindrical Langmuir probe, one should obtain the plasma solution around the biased probe [6,7].

The problem of the plasma-sheath transition is still the

subject of numerous recent investigations [8–11]. This is partly due to the singularity caused by the representations of various effects (collision, space charge and ion temperature). The variations of the plasma variables in the plasma-wall transition region can be characterized with several scale lengths [12]. The ionization length or the ion mean free path can be used for observing the variations of plasma variables in the presheath region. On the other hand, the electron Debye length can be used as a scale length for the sheath region because the sheath width extends only a few electron Debye lengths [13]. The evolutions of plasma variables in the presheath region can be represented more clearly with the scale length of the ionization length.

The theoretical model for the sheath structure of cylindrical and spherical probes immersed in low-pressure electronegative plasmas has been developed by several authors [8,9,14–19]. The use of the plasma approximation in the presheath region has produced rich theoretical observations of the oscillatory electric potential and stratified presheath [15–22]. Some authors have insisted that these oscillations can be attenuated with consideration of collisions and finite thermal motion of positive ions [15].

---

\*E-mail: thchung@dau.ac.kr

In a previous paper [23], a fluid model for collisionless plasmas with cold positive ions was developed for studying the structure of the plasma-wall boundary in low-pressure electronegative plasmas. Similar issues have also been analyzed by several authors [19,20,22,24–26]. In this study, the model is extended to include collisions and the finite thermal motion of positive ions. The spatial distributions of the electric potential and of the velocity and density of positive ions are calculated in the surroundings of a negatively-biased cylindrical probe immersed in an electronegative plasma. The control parameters are the ratio of the negative ion density to the electron density, the ratios of the electron temperature to the positive and the negative ion temperatures and the ratio of the momentum transfer collision frequency to the ionization frequency.

In contrast to the previous work [13], the model equations in this study are solved on the scale of the ionization length. In that paper, there were some misleading arguments concerning the behavior of the sheath width as functions of the control parameters. One of aims of this work is to correct that. Moreover, a calculation of plasma variables on the scale of the ionization length allows us to determine more obviously the position of the sheath edge and the positive ion velocity at the sheath edge. Therefore, the physical nature of the plasma sheath boundary is more clearly described. From the calculated results, the position of the sheath edge, the positive ion velocity at sheath edge and the positive ion current collected by the probe are determined and compared with analytic (or scaling) formulas. Especially, the effects of these control parameters on the positive ion current collected by the probe are investigated. The effect of the non-neutrality parameter, defined as the ratio between the electron Debye length and the ionization length, is also discussed. Finally, the validity of the plasma approximation in the presheath region is discussed.

## II. FORMULATION

A fluid model is developed without the quasi-neutral approximation to solve for the spatial distributions of electric potential and of the density and velocity of positive ions in the surroundings of a cylindrical probe immersed in an electronegative plasma. A set of coupled equations are formulated, including the steady-state fluid equations of continuity and motion for the positive ion and Poisson's equation with Boltzmann electrons and Boltzmann negative ions [15, 16]. The assumption of Boltzmann negative ions is valid for negative ions so long as the wall losses dominate volume recombination.

The plasma variables are calculated along the distance from the plasma region to any arbitrary small distance near the probe edge. For simplicity, the electronegative plasma is assumed to consist of three charged species, which are positive ions, negative ions and electrons. The

basic equations for the positive ions are the continuity equation,

$$\nabla \cdot [n_+ \mathbf{v}_+] = \nu_{iz} n_e, \quad (1)$$

and the equation of momentum transfer,

$$m_+ n_+ \mathbf{v}_+ \cdot \nabla \mathbf{v}_+ = e n_+ \mathbf{E} - \nabla p_+ - m_+ n_+ \nu_c \mathbf{v}_+, \quad (2)$$

where  $n_+$ ,  $m_+$ ,  $p_+$  and  $\mathbf{v}_+$  are the density, the mass, the pressure and the velocity of a positive ion, respectively,  $n_e$  is the electron density,  $\nu_{iz}$  and  $\nu_c$  are the ionization frequency and the momentum-transfer collision frequency, respectively and  $\mathbf{E}$  is the electric field. In Eq. (2) the ionization source term is not included because a small drag force due to collisions between positive ions and neutrals is considered in this work [16].

Poisson's equation is written as

$$\varepsilon_0 \nabla \cdot \mathbf{E} = e (n_+ - n_e - n_-), \quad \mathbf{E} = -\nabla V, \quad (3)$$

where  $\varepsilon_0$  is the permittivity of the vacuum,  $n_-$  is the negative ion density,  $e$  is the electron charge and  $V$  is the electric potential. Electrons and negative ions are assumed to follow the Boltzmann energy distribution:

$$n_e = n_{e0} \exp\left(\frac{eV}{kT_e}\right), \quad (4)$$

$$n_- = n_{-0} \exp\left(\frac{eV}{kT_-}\right), \quad (5)$$

where  $T_e$  and  $T_-$  are the temperatures of the electrons and the negative ions, respectively and  $k$  is the Boltzmann constant. The subscript 0 indicates the value at the plasma region. In order for the Boltzmann relation for negative ions to hold, the condition

$$\Gamma_- \ll D_- \frac{dn_-}{dr} \quad (6)$$

must hold. Neglecting the recombination the negative ion flux is written as

$$\Gamma_- = \int K_{att} n_e n_g dr, \quad (7)$$

where  $D_-$ ,  $K_{att}$  and  $n_g$  are the diffusion coefficient of negative ions, the attachment coefficient and the neutral gas density, respectively. The validity of this condition will be discussed in Section III.

The model equations can be written in cylindrical coordinates with the assumption that positive ions move radially towards the probes.

$$\frac{d}{dr} n_+ v_+ + \frac{n_+ v_+}{r} = \nu_{iz} n_e, \quad (8)$$

$$m_+ n_+ v_+ \frac{dv_+}{dr} = -e n_+ \frac{dV}{dr} - \frac{dp_+}{dr} - m_+ n_+ \nu_c v_+, \quad (9)$$

$$\varepsilon_0 \left( \frac{d^2 V}{dr^2} + \frac{1}{r} \frac{dV}{dr} \right) = -e (n_+ - n_e - n_-), \quad (10)$$

where  $r$  denotes the radial position in cylindrical coordinates with the origin at the center of the probe. The momentum-transfer collision frequency is written as

$$\nu_c = n_g \sigma (v_+) v_+, \quad (11)$$

where  $\sigma(v_+)$  is the momentum transfer collision cross section for collisions between positive ions and neutrals. Elastic and charge-exchange collisions contribute to this cross section. We assume that this cross section has a power-law dependence on the positive ion speed of the form

$$\sigma(v_+) = \sigma_s \left( \frac{v_+}{c_s} \right)^\gamma, \quad (12)$$

where  $c_s$  is the Bohm velocity ( $=\sqrt{kT_e/m_+}$ ),  $\sigma_s$  is the cross section at that speed and  $\gamma$  is the dimensionless parameter ranging from 0 to  $-1$  [27]. The case of  $\gamma = 0$  corresponds to a constant cross section and the case of  $\gamma = -1$  to a constant collision frequency. A constant collision frequency ( $\gamma = -1$ ) is employed throughout this study. The numerical calculation for arbitrary  $\gamma$  (rather than  $-1$ ) can be pursued without difficulty with some modifications in the collision term of the momentum balance equation.

The solution of the model equations describes the structure of the sheath (and presheath) region around a cylindrical electrode. We use the following dimensionless variables and parameters:

$$\xi = \frac{r}{\Lambda}, \quad \tilde{n} = \frac{n_+}{n_{e0}}, \quad u = -\frac{v_+}{c_s}, \quad \eta = -\frac{eV}{kT_e}, \quad (13)$$

$$\alpha_0 = \frac{n_{-0}}{n_{e0}}, \quad \gamma_- = \frac{T_e}{T_-}, \quad \gamma_+ = \frac{T_e}{T_+}, \quad q = \frac{\lambda_D}{\Lambda}, \quad \delta = \frac{\nu_c}{\nu_{iz}}.$$

where  $\lambda_D$  is the electron Debye length,  $\Lambda = c_s/\nu_{iz}$  is the ionization length and  $T_+$  is the temperature of positive ions. The ionization length determines the overall widths of the presheath region (and the sheath region). The presheath width scales similar to the ionization length. The  $q$  is sometimes called the non-neutrality parameter. For a fixed positive ion density, as the electronegativity is increased, the Debye length increases due to a decrease in electron density, thus resulting in a larger  $q$ . The neutral gas density and the temperatures of the electrons and negative ions are taken as constant and an isothermal positive ion flow is assumed.

The dimensionless equations of ion continuity and momentum balance for positive ions and Poisson's equation are written as

$$\frac{d}{d\xi}(\tilde{n}u) + \frac{\tilde{n}u}{\xi} = -e^{-\eta}, \quad (14)$$

$$\left( u - \frac{1}{\gamma_+ u} \right) \frac{du}{d\xi} = \frac{d\eta}{d\xi} + \frac{1}{\gamma_+ \xi} + \frac{e^{-\eta}}{\gamma_+ \tilde{n}u} + u\delta, \quad (15)$$

$$q^2 \left( \frac{d^2\eta}{d\xi^2} + \frac{1}{\xi} \frac{d\eta}{d\xi} \right) = \tilde{n} - e^{-\eta} - \alpha_0 e^{-\gamma_- \eta}. \quad (16)$$

These three first-order nonlinear differential equations are solved numerically to obtain the evolutions of the plasma variables along the distance from the plasma region to the probe surface.

The assumption  $\lambda_D \ll \Lambda$  clearly corresponds to  $q \ll 1$ . In the asymptotic limit  $q \rightarrow 0$ , Poisson equation is replaced with the quasi-neutrality, resulting in the plasma

approximation. For the plasma approximation  $q = 0$ , these equations describe a charge-neutral plasma with a sheath of zero thickness. The plasma solution becomes singular at the sheath-plasma boundary because the sheath is not charge neutral [16]. On the presheath scale, the sheath is infinitely thin and the sheath edge is defined by a field singularity  $\frac{d\eta}{d\xi} \rightarrow \infty$ . Eq. (15) shows that the plasma equation is singular at the point where  $u^2 = 1/\gamma_+$ , regardless of collisions. This indicates that the Bohm criterion is not much modified, regardless of collisions [28].

If current continuity is assumed, we have a conserved quantity

$$\xi \tilde{n}u = I. \quad (17)$$

Then, the Poisson equation can be replaced with

$$q^2 \left( \frac{d^2\eta}{d\xi^2} + \frac{1}{\xi} \frac{d\eta}{d\xi} \right) = \frac{I}{u\xi} - e^{-\eta} - \alpha_0 e^{-\gamma_- \eta}. \quad (18)$$

This equation, combined with the equation of motion, Eq. (15), with  $\gamma_+ \rightarrow \infty$  and  $\delta = 0$ , has been used to obtain the theoretical  $I - V$  characteristic curve of the probe [6,7]. This is an extension of the cold-ion theory of Allen-Boyd-Reynolds (ABR) [29-31].

In the quasi-neutral region, the differential term of the Poisson equation, Eq. (18), may be neglected. Then, we have

$$\frac{I}{u\xi} - e^{-\eta} - \alpha_0 e^{-\gamma_- \eta} = 0. \quad (19)$$

Using Eq. (19) and its differentiation with respect to  $\xi$ , we can eliminate  $\xi$  and  $d\eta/d\xi$  from Eq. (15) to obtain

$$\left( u + \frac{I\delta}{u(e^{-\eta} + \alpha_0 e^{-\gamma_- \eta})} \right) \frac{du}{d\eta} = 1 + \frac{1}{\gamma_+} \frac{e^{-\eta} + \alpha_0 \gamma_- e^{-\gamma_- \eta}}{e^{-\eta} + \alpha_0 e^{-\gamma_- \eta}} + \frac{I\delta(e^{-\eta} + \alpha_0 \gamma_- e^{-\gamma_- \eta})}{(e^{-\eta} + \alpha_0 e^{-\gamma_- \eta})^2}. \quad (20)$$

It should be noted that the velocity of positive ions entering the presheath depends on  $\alpha_0$ ,  $\delta$ ,  $\gamma_+$ ,  $\gamma_-$  and  $I$  (the positive ion current). Integrating this equation with the initial condition  $u = 0$  at  $\eta = 0$ , we obtain  $u$  as a function of  $\eta$ . The integration needs a fixed value of  $I$ .

Figure 1 shows the evolution of  $u$  with  $\eta$  for various  $\alpha_0$  and  $I$ . The evolution of  $u$  with  $\eta$  has a sensitive dependence on  $\alpha_0$ . With larger values of  $\alpha_0$ , positive ions can be accelerated steeply in the presheath. With smaller values of  $I$ , positive ions can be accelerated steeply. However, the values of  $\gamma_+$  and  $\gamma_-$  have insignificant influence on the evolution of  $u$  with  $\eta$ . These provide the initial conditions to the model equations, Eqs. (14)-(16). With Eq. (20), typical initial values are chosen as  $\eta = 0.0236$  and  $u = 0.1806$  (assuming  $I = 0.72$ ,  $\delta = 0.01$ ,  $\gamma_+ = 30$ ,  $\gamma_- = 10$  and  $\alpha_0 = 2$ ) and according to Eq. (19), the value of  $\xi$  satisfying this condition is 1.794. The initial

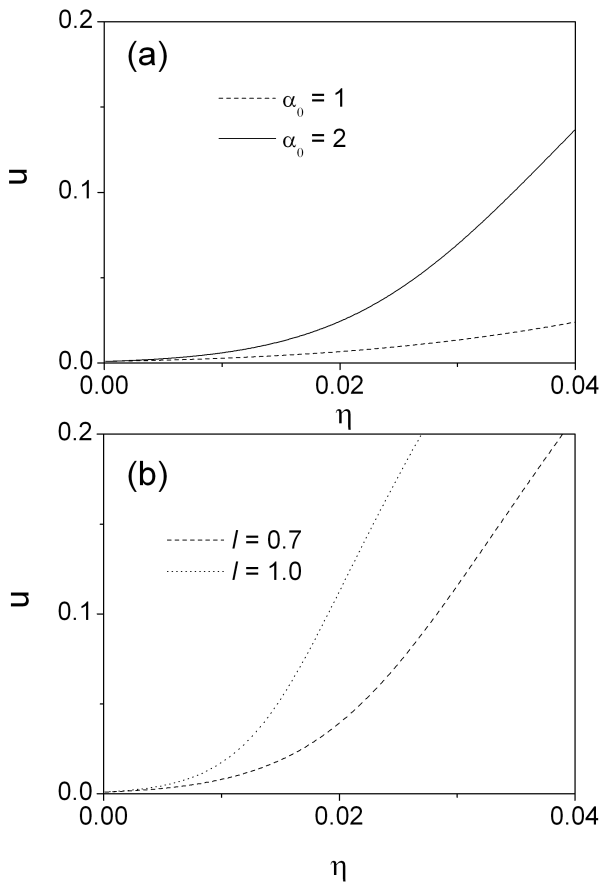


Fig. 1. The evolution of  $u$  with  $\eta$  near the plasma sheath transition region for (a) two  $\alpha_0$  and (b) two  $I$ , where  $\gamma_+ = 30$ ,  $\gamma_- = 10$ ,  $\delta = 0.1$  and  $I = 0.5$  for (a) and  $\alpha_0 = 5$  for (b).

value of  $\xi$  varies depending on the control parameters and becomes 0.9739 when  $\alpha_0 = 5$ . The initial value of the normalized density is assumed to be  $\tilde{n} = 1 + \alpha_0$ .

In this work, the sheath refers to the region surrounding the probe where positive space charge exists; that is, this region includes the ion sheath where the electron density is negligible and the transition region where the electron density cannot be neglected, but quasineutrality can never be applied [32]. The sheath edge marks the point where quasineutrality breaks and where the electric potential rises to infinity at that point as mentioned before. The location of the sheath edge and the calculated values of the density and the velocity of positive ions give the positive ion current to the probe.

### III. RESULTS AND DISCUSSION

The main focus of this paper is to investigate the effects of collisions and finite thermal motions of positive ions and negative ions on the positive ion current to the probe and on the position of sheath edge. In order to examine these, the spatial distributions of the electric

potential and of the density and the velocity of positive ions should be obtained. For that purpose, Eqs. (14)-(16) are solved numerically by using the fourth-order Runge-Kutta method with the initial condition, which is obtained by solving the quasi-neutral equations, Eqs. (19) and (20).

It is very difficult to integrate Eqs. (14)-(16) from  $\xi = \infty$ . Instead, a choice of  $\xi = 1.0$  as a start from the plasma region is made based on the fact that  $\Lambda$  is much larger than the sheath width. We have tried several values for the upper limit of integration and found that the numerical solutions are quite stable and reasonable for the choice of 1.0  $\Lambda$ . Except for very small or large values of  $\xi$  for the initial condition (upper limit), the choice of the upper limit does not much affect the location of sheath edge and the positive ion current to the probe.

As an example of the electronegative plasma, we can consider an oxygen discharge with  $p = 10$  mTorr and  $T_e = 4$  eV. We have  $c_s = 3 \times 10^5$  cm/s,  $\nu_{iz} = 10^6$  1/s and  $\Lambda = 0.3$  cm. On the presheath scale Eq. (6) can be written as

$$\Lambda^2 \ll \frac{D_- n_-}{K_{att} n_g n_e}. \quad (21)$$

For the oxygen discharge above with  $K_{att} = 10^{-10}$  cm<sup>3</sup>/s,  $D_- = 3000$  cm<sup>2</sup>/s and a moderate value of  $\alpha_0$ , this condition is easily fulfilled and the Boltzmann relation for negative ions is valid.

The spatial distributions of the normalized potential, the normalized density and the normalized velocity and flux of positive ions entering the probe are calculated for various values of  $q$ ,  $\alpha_0$ ,  $\delta$ ,  $\gamma_+$  and  $\gamma_-$ . Especially, the effects of the control parameters  $\gamma_+$ ,  $\gamma_-$ ,  $\delta$ ,  $\alpha_0$  and  $q$  on the radial profiles of the electric potential and of the velocity and density of positive ions toward the probe are investigated.

In most of parameter region of this study, the solutions of the model equations, Eqs. (14)-(16), have oscillatory structures. These oscillations occur because quasineutrality is violated while the positive ions do not satisfy the Bohm criterion [16]. The average potential continues to increase during the oscillations. After a number of oscillations, the Bohm criterion is satisfied and a sheath forms. However, such stationary potential oscillations are artifacts inherent to the fluid theory [15,17,33]. Also, incomplete initial conditions for solving the coupled fluid equations might give rise to the oscillations. As long as the plasma approximation is assumed in the plasma sheath transition region, the space-charge oscillations are accompanied by a double layer (or stratified presheath) [34,35]. However, the spatial oscillations shown in the solutions of the model equations have a slightly different nature than those associated with a double layer. In this work, the spatial oscillations occur due to the characteristics of the fluid equation and its sensitive dependence on the initial condition. However, if the initial condition with  $\frac{d\eta}{d\xi}$  equal to 0 at  $\xi = 1$  is used, no spatial oscillations are observed. Thus, in order to fully address the

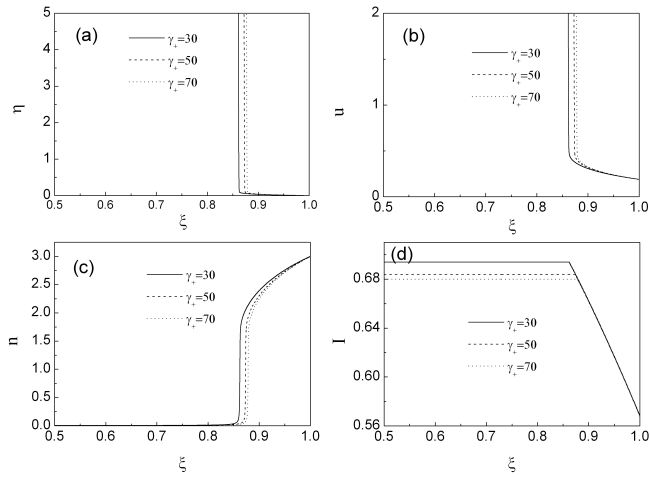


Fig. 2. (a) Normalized potential, (b) normalized velocity, (c) normalized density and (d) normalized current of positive ions along the normalized distance for various positive ion temperatures ( $\gamma_+ = 30, 50$  and  $70$ ). Here,  $q = 0.0002$ ,  $\alpha_0 = 2$ ,  $\gamma_- = 10$  and  $\delta = 0.5$ .

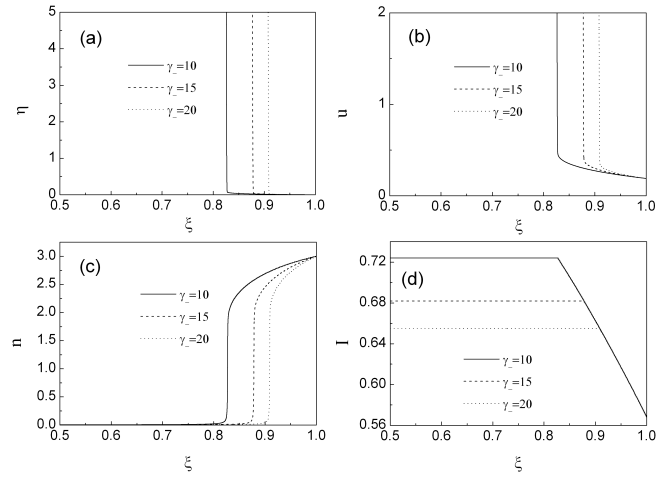


Fig. 3. (a) Normalized potential, (b) normalized velocity, (c) normalized density and (d) normalized current of positive ions along the normalized distance for various negative ion temperatures ( $\gamma_- = 10, 15$  and  $20$ ). Here,  $q = 0.0002$ ,  $\alpha_0 = 2$ ,  $\gamma_+ = 30$  and  $\delta = 0$ .

purpose of this work, the initial condition of  $\frac{d\eta}{d\xi} = 0$  at  $\xi = 1$  is used throughout the study, getting rid of the spatial oscillations of the plasma variables.

Figures 2(a) and 2(b) show the normalized potential and the normalized velocity of positive ions along the distance from the plasma ( $\xi = 1.0$ ) to the probe ( $\xi$  approaches zero) for various values of  $\gamma_+$  with  $q = 0.0002$ . Although  $\xi$  is cut off at 0.5 in the figures, the calculation proceeds up to zero. As  $\gamma_+$  increases (as the positive ion temperature becomes lower), the sheath edge ( $\xi_s$ ) is located at a larger value from the center of the probe. Here, the sheath edge can also be defined as either the point at which the electric potential becomes infinite or the point at which the positive ions reach the speed of sound in the medium (the supersonic ion criterion) [7]. Since the sheath edge is defined by a field singularity and the sheath is infinitely thin on the presheath scale, we assume that the sheath width behaves similar to the presheath width, which is the distance from the plasma ( $\xi = 1$  in this work) to the sheath edge.

For electronegative plasmas with collisionless and cold positive ions, the Bohm criterion becomes

$$u_s^2 \geq \frac{1 + \alpha_s}{1 + \alpha_s \gamma_-}, \quad (22)$$

where subscript  $s$  means the value at the sheath edge. This condition can be written as

$$u_s^2 \geq \frac{1}{1 - \frac{\alpha_0}{1 + \alpha_0}(1 - \gamma_-)}, \quad (23)$$

which has been justified by different methods, including the Sagdeev potential or the requirement of zero derivatives of space charge at the sheath-presheath edge with respect to the potential [36–38].

The effect of  $\gamma_+$  on the  $u_s$  (the positive ion velocity at the sheath edge) behaves similarly as that of  $\gamma_-$ . As the  $\gamma_+$  increases, the positive ion velocity at the sheath edge is observed to decrease and the sheath width to decrease. From the figure, it can be noted that if the positive ions have larger thermal motion, the sheath is increased and the positive ion current collected by the probe increases [26].

Figure 2(c) shows the normalized density of positive ions along the distance for various parameter values of  $\gamma_+$ . The density profile of positive ion is observed to decrease rapidly toward the probe as  $\gamma_+$  increases. Figure 2(d) shows the calculated  $\xi \tilde{n} u (= I(\xi))$  representing the normalized positive ion current. The results indicate that as  $\gamma_+$  increases, the positive ion current collected by the probe decreases. The calculated  $I(\xi)$  is observed to remain constant throughout the sheath region; therefore,  $I$  in Eq. (20) can be considered a constant. This allows the ABR theory to be valid for most of parameter region of interest. The location of the sheath edge can be found to be consistent in (a)-(d) of Figure 2. The normalized positive ion current collected by the probe is  $\xi_s \tilde{n}_s u_s$  ( $s$  denotes the value at the sheath edge).

Figures 3(a) and 3(b) show the normalized potential and the normalized velocity of positive ions along the distance from the plasma to the probe for various values of  $\gamma_-$ . As the  $\gamma_-$  increases from 10 to 20, the positive ion velocity at the sheath edge is observed to decrease, in agreement with Eq. (23) and the sheath width observed to decrease. Figures 3(c) and 3(d) show the normalized density of positive ions and the calculated  $\xi \tilde{n} u (= I(\xi))$  along the distance. The profiles are observed to have the same tendencies as those in Figure 2. However, the value of  $\gamma_-$  has more significant effects than that of  $\gamma_+$ .

Figures 4(a) and 4(b) show the normalized potential

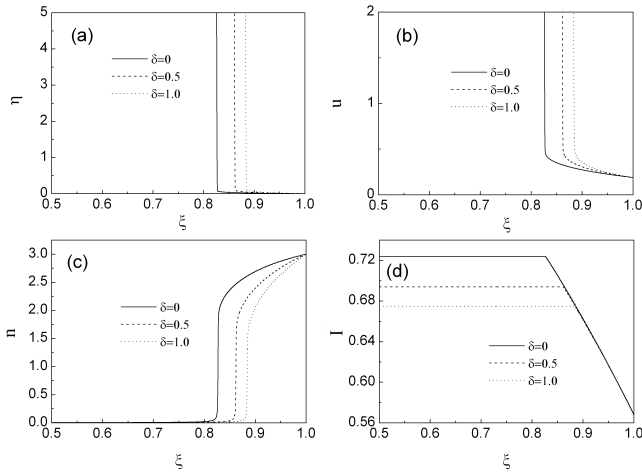


Fig. 4. (a) Normalized potential, (b) normalized velocity, (c) normalized density and (d) normalized current of positive ions along the normalized distance for various collision parameters ( $\delta = 0, 0.5$  and  $1$ ). Here,  $q = 0.0002$ ,  $\alpha_0 = 2$ ,  $\gamma_- = 10$  and  $\gamma_+ = 30$ .

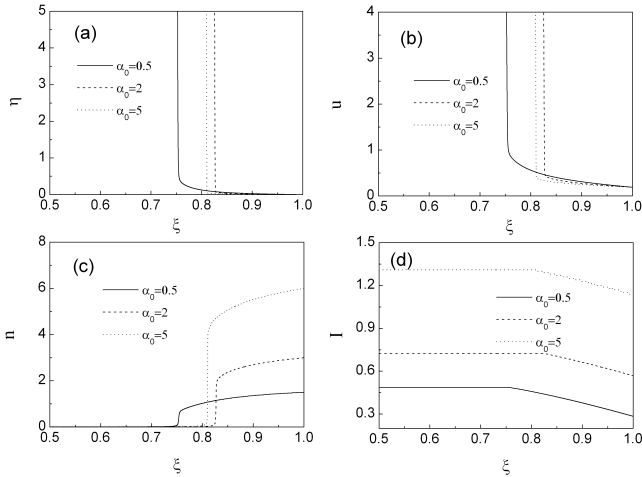


Fig. 5. (a) Normalized potential, (b) normalized velocity, (c) normalized density and (d) normalized current of positive ions along the normalized distance for various  $\alpha_0$  ( $\alpha_0 = 0.5, 2$  and  $5$ ). Here,  $q = 0.0002$ ,  $\gamma_- = 10$ ,  $\gamma_+ = 30$  and  $\delta = 0$ .

and the normalized velocity of positive ions along the distance for various  $\delta$  at  $q = 0.0002$ . The  $\delta$  indicates the ratio of the momentum transfer collision frequency to the ionization frequency. This value defines the collisionality of the plasma and is small at low pressure, being less than 1 [28,33]. As  $\delta$  increases, the sheath edge approaches the plasma region. As shown,  $u_s$  decreases as  $\delta$  increases. The increase in  $\delta$  (collision term) causes the electric potential and the velocity to increase more rapidly going from the plasma to the probe.

Figure 4(c) shows the normalized density of positive ions along the distance for various  $\delta$ . It is observed that the density profile of positive ion decreases drastically toward the probe as  $\delta$  increases. Figure 4(d) shows the

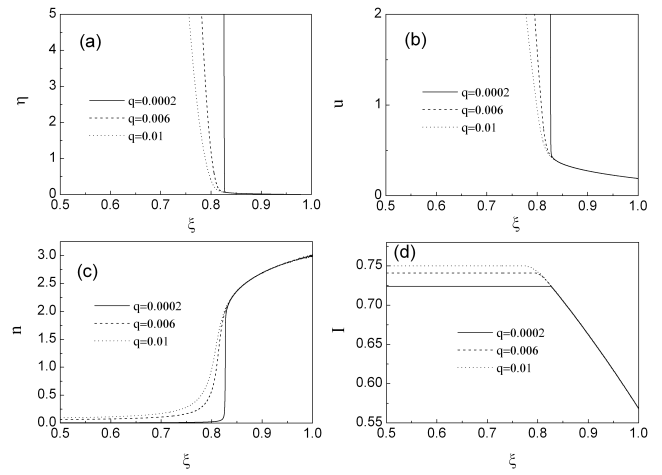


Fig. 6. (a) Normalized potential, (b) normalized velocity, (c) normalized density and (d) normalized current of positive ions along the normalized distance for various  $q$  ( $q = 0.0002, 0.006$  and  $0.01$ ). Here,  $\alpha_0 = 2$ ,  $\gamma_- = 10$ ,  $\gamma_+ = 30$  and  $\delta = 0$ .

calculated  $I(\xi)$  for several  $\delta$ . The results show that the positive ion current to the probe decreases as  $\delta$  increases.

The normalized potential and the normalized velocity of positive ions corresponding to the three different  $\alpha_0$  are shown in Figures 5(a) and 5(b). As  $\alpha_0$  increases, the potential increases rapidly to higher values and the sheath width decreases. This result is in agreement with the results of Crespo *et al.* [7] and Amemiya *et al.* [14]. As the  $\alpha_0$  increases, the positive ion velocity at the sheath edge is observed to decrease, in agreement of Eq. (23). Figure 5(c) shows the density profiles of positive ions for various  $\alpha_0$ . Toward the probe, the density profile of positive ions is observed to decrease more drastically for higher values of  $\alpha_0$ . From Figure 5(d), one sees that the positive ion current collected by the probe increases with increasing  $\alpha_0$  because the initial value of the normalized density is  $1 + \alpha_0$ . However, if a positive ion density ( $n_{+0}$ ) is fixed, with a normalization by  $1 + \alpha_0$ , the results indicate that a lower  $\alpha_0$  case produces a larger positive ion current.

Figures 6(a) and 6(b) show the profiles of the electric potential and of the normalized velocity of positive ions for three different  $q$ . As  $q$  increases, the slopes of the electric potential and the velocity decrease, indicating that the condition of a field singularity  $\frac{d\eta}{d\xi} \rightarrow \infty$  is alleviated. One should note that it is difficult to observe the effect of  $q$  on the positive ion velocity at the sheath edge and the sheath width because coordinate  $\xi$  itself depends on the  $q$  value in this formulation. However, physically, as  $q$  increases, more charged species are produced; thus, the electric potential increases more rapidly (going from the plasma to the probe) and the sheath width decreases. Figure 6(c) shows the normalized density of positive ions along the distance for various  $q$ . From Figure 6(d), the positive ion current collected by the probe is seen to increase with increasing  $q$  because larger  $q$  results in more

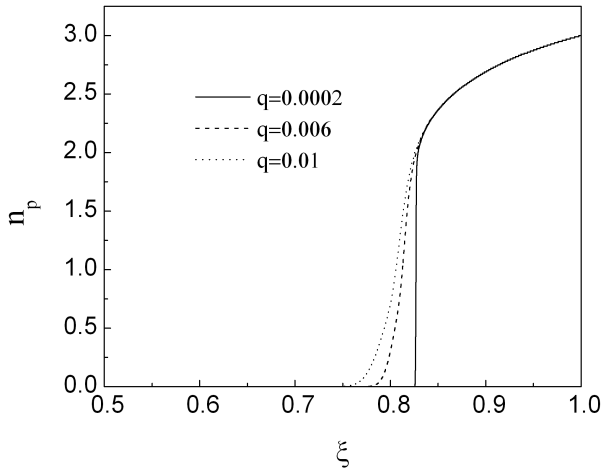


Fig. 7. Normalized density profiles of positive ions calculated by using the plasma approximation ( $\tilde{n} = e^{-\eta} + \alpha_0 e^{-\gamma-\eta}$ ) for various  $q$  values.

positive ion production by ionization.

Figure 7 shows the normalized density profiles of positive ions calculated by the plasma approximation ( $\tilde{n} = e^{-\eta} + \alpha_0 e^{-\gamma-\eta}$ ) for various  $q$  values. These are compared with Figure 6(c). As  $q$  increases, the deviation from the plasma approximation increases. A variety of rich physics issues relating to the oscillatory potential and to the stratified sheath stems from the adoption of the plasma approximation in the presheath region [15–22]. However, the calculation of this work indicates that a deviation from the plasma approximation becomes significant even at  $q = 0.006$ , which is a typical case for high density electronegative plasmas and that the plasma approximation is no longer valid except for plasmas with the  $q$  less than 0.0005. One should note that the applicability of this model is limited to the case of thin sheaths where the electron Debye length is much lower than the probe radius because this model neglects the orbital motion of the ions. Moreover, the probe radius should not be too small compared to the ionization length. When  $r_p \ll \Lambda$ , it governs the size of presheath and collisions (and ionization) play little role. As the value of  $q$  increases, the sheath width decreases, so this model cannot explain the positive ion collection by the probe in a large  $q$  region. Therefore, the analysis of this study is valid in only an appropriate range of the  $q$  value.

In relation with the probe experiment, one application of this formulation is to find the ionization rate of the plasma. The positive ion saturation current is written as

$$I_+ = 2\pi e r_s n_{+s} v_{+s} = 2\pi e \Lambda n_{e0} c_s I. \quad (24)$$

The electron density  $n_{e0}$  and the electron temperature (thus  $c_s$ ) are supposed to be determined from the electron saturation current and the slope of the experimental  $I-V$  curve of the probe in the exponential region. If  $\alpha_0$ ,  $\gamma_{\pm}$  and  $\delta$  can be known or assumed, then we can estimate the  $\Lambda$  value (thus the ionization rate) of the plasma by

carefully comparing  $I_+$  and  $I$ .

Although this model can give quite a clear picture of the sheath region and the location of the sheath edge for various sets of plasma parameters and can allow us to estimate the positive ion current easily, this model has some drawback in predicting the probe  $I-V$  characteristics accurately. For one, the model in the present work may not precisely describe the ion motion in the sheath region because the assumptions made in formulating the model equations and the condition of constant parameters might not be valid in the sheath region. In addition, one should note that a kinetic analysis has to be performed to take into account the effects of ion orbital motion, ion trapping in the sheath and the finite length of the cylindrical probe because in the collisional limit, the correct expression for the ion saturation current for a cylindrical probe should contain a logarithmic term accounting for the finite length of the probe.

#### IV. CONCLUSION

The spatial distributions of the electric potential and of the velocity and density of positive ions are calculated in the surroundings of a negatively-biased cylindrical probe immersed in an electronegative plasma. The control parameters are the ratio of the negative ion density to the electron density, the ratios of the electron temperature to the positive and the negative ion temperatures and the ratio of the rate coefficient for the momentum transfer collision to that for the ionization. The model equations are solved on the scale of the ionization length. The position of the sheath edge ( $\xi_s$ ), the positive ion velocity at the sheath edge ( $u_s$ ) and the positive ion current ( $\xi_s \tilde{n}_s u_s$ ) collected by the probe are determined and compared with the results from analytic (or scaling) formulas. The effects of the control parameters on the positive ion velocity at the sheath edge and on the position of the sheath edge (and sheath width) are discussed. The position of the sheath edge determines the sheath area for positive ion collection. The results of the calculation are consistent with the results from the analytic (or scaling) formulas. If positive (and negative) ions have a larger thermal motion, the positive ion velocity at the sheath edge, the sheath and the positive ion current collected by the probe increase. An increase in the number of collision causes the positive ion velocity at the sheath edge to decrease and the sheath to decrease, resulting in a decrease in the positive ion current. An increase in electronegativity ( $\alpha_0$ ) causes the positive ion velocity at sheath edge to decrease and the sheath width to decrease, resulting in an increase in the positive ion current. As the value of the non-neutrality parameter  $q$  increases, the positive ion current collected by the probe increases. The deviation from the plasma approximation is observed to become significant even at  $q = 0.006$ , which is a typical case for high-density elec-

tronegative plasmas and the plasma approximation is no longer valid, except for plasmas with  $q$  less than 0.0005. The merit of this model lies in its giving a clear picture of the plasma sheath boundary and a straight-forward calculation of the positive ion current collected by the probe.

### ACKNOWLEDGMENTS

This work was supported by the research grant of Dong-A University.

### REFERENCES

- [1] T. H. Chung, H. J. Yoon and D. C. Seo, *J. Appl. Phys.* **86**, 3536 (1999).
- [2] T. H. Chung, D. C. Seo, G. H. Kim and J. S. Kim, *IEEE Trans. Plasma Sci.* **29**, 970 (2001).
- [3] D. C. Seo, T. H. Chung, H. J. Yoon and G. H. Kim, *J. Appl. Phys.* **89**, 4218 (2001).
- [4] E. Stamate and K. Ohe, *J. Appl. Phys.* **84**, 2450 (1998).
- [5] E. Stamate and K. Ohe, *J. Appl. Phys.* **89**, 2058 (2001).
- [6] R. M. Crespo, J. I. F. Palop, M. A. Hernandez and J. Ballesteros, *J. Appl. Phys.* **95**, 2982 (2004).
- [7] R. M. Crespo, J. I. F. Palop, M. A. Hernandez, S. B. del Pino and J. Ballesteros, *J. Appl. Phys.* **96**, 4777 (2004).
- [8] K. U. Riemann, J. Seebacher, D. D. T. Sr. and S. Kuhn, *Plasma Phys. Control. Fusion* **47**, 1949 (2005).
- [9] J. Kim, C. Na, D. Lee, N. M. Becker, M. Cho and W. Namkung, *J. Korean Phys. Soc.* **53**, 3758 (2008).
- [10] M. H. Lee, I. J. Choe and C. W. Chung, *J. Korean Phys. Soc.* **51**, 1307 (2007).
- [11] T. Kim and M. J. Lee, *J. Korean Phys. Soc.* **53**, 636 (2008).
- [12] K. U. Riemann, *IEEE Trans. Plasma Sci.* **23**, 709 (1995).
- [13] T. H. Chung, *J. Appl. Phys.* **103**, 123302 (2008).
- [14] H. Amemiya, B. M. Annaratone and J. E. Allen, *Plasma Sources Sci. Technol.* **8**, 179 (1999).
- [15] R. N. Franklin, *Plasma Sources Sci. Technol.* **9**, 191 (2000).
- [16] T. E. Sheridan, P. Chabert and R. W. Boswell, *Plasma Sources Sci. Technol.* **8**, 457 (1999).
- [17] A. Kono, *J. Phys. D: Appl. Phys.* **32**, 1357 (1999).
- [18] A. Kono, *J. Phys. D: Appl. Phys.* **34**, 1083 (2001).
- [19] A. Kono, *J. Phys. D: Appl. Phys.* **36**, 465 (2003).
- [20] J. I. F. Palop, J. Ballesteros, M. A. Hernandez, R. M. Crespo and S. B. del Pino, *J. Phys. D: Appl. Phys.* **37**, 863 (2004).
- [21] J. I. F. Palop, J. Ballesteros, M. A. Hernandez and R. M. Crespo, *Plasma Sources Sci. Technol.* **16**, S76 (2007).
- [22] J. I. F. Palop, J. Ballesteros, M. A. Hernandez, R. M. Crespo and S. B. del Pino, *J. Phys. D: Appl. Phys.* **38**, 868 (2005).
- [23] T. H. Chung, *Phys. Plasmas* **13** 024501 (2006).
- [24] J. I. F. Palop, J. Ballesteros, R. M. Crespo and M. A. Hernandez, *Appl. Phys. Lett.* **88**, 261502 (2006).
- [25] R. M. Crespo, J. I. F. Palop, M. A. Hernandez, S. B. del Pino, J. M. Diaz-Cabrera and J. Ballesteros, *J. Appl. Phys.* **99**, 053303 (2006).
- [26] J. I. F. Palop, J. Ballesteros, M. A. Hernandez, R. M. Crespo and S. B. del Pino, *J. Appl. Phys.* **95**, 4585 (2004).
- [27] T. E. Sheridan and J. Goree, *Phys. Fluids B* **3**, 2796 (1991).
- [28] R. N. Franklin, *J. Phys. D: Appl. Phys.* **36**, 2821 (2003).
- [29] J. E. Allen, R. L. F. Boyd and P. Reynolds, *Proc. Phys. Soc. London. Sect. B* **70**, 297 (1957).
- [30] F. F. Chen, *J. Nucl. Energy, Part C* **7**, 47 (1965).
- [31] J. I. F. Palop, J. Ballesteros, V. Colomer and M. A. Hernandez, *J. Phys. D: Appl. Phys.* **29**, 2832 (1996).
- [32] F. Iza and J. K. Lee, *J. Vac. Sci. Technol. A* **24**, 1366 (2006).
- [33] R. N. Franklin and J. Snell, *J. Phys. D: Appl. Phys.* **33**, 1990 (2000).
- [34] T. E. Sheridan, N. St. J. Braithwaite and R. W. Boswell, *Phys. Plasmas* **6**, 4375 (1999).
- [35] T. E. Sheridan, *J. Phys. D: Appl. Phys.* **32**, 1761 (1999).
- [36] K. Yasserian, M. Aslaninejad, M. Ghorannesviss and F. M. Aghamir, *J. Phys. D: Appl. Phys.* **41**, 105215 (2008).
- [37] N. St. J. Braithwaite and J. E. Allen, *J. Phys. D: Appl. Phys.* **21**, 1733 (1988).
- [38] M. A. Lieberman and A. J. Lichtenberg, *Principles of Plasma Discharge and Materials Processing* (Wiley, New York, 1994), p. 168.